

A new Parameterization for the Pion Vector Form Factor

C. Hanhart

*Institut für Kernphysik, Institute for Advanced Simulation and Jülich Center for Hadron Physics,
Forschungszentrum Jülich, D-52425 Jülich, Germany*

Abstract

A new approach to the parameterization of pion form factors is presented and for illustration applied to the pion vector form factor. It has the correct analytic structure, is at low energies consistent with recent high accuracy analyses of $\pi\pi$ scattering phase shifts and, at high energies, maps smoothly onto the well-known, successful isobar model.

Key words: Pion form factor, Omnès representation, 11.55.Bq, 13.40.Gp

1. Introduction

In recent years the knowledge about the low energy two-pion system has improved significantly, both experimentally as well as theoretically: for the low partial waves phase shift parameterizations of high accuracy exist from different dispersive analyses, either involving data only [1], or involving both data as well as constraints from chiral symmetry [2]. The analyses are based on Roy or Roy-type equations that respect analyticity as well as crossing symmetry. Especially, left-hand cuts are included without approximation.

In contrast to this, pion form factors or production reactions are often modeled either by sums of Breit-Wigners or improved versions thereof [3–5] or by the K-matrix formalism. In case of overlapping resonances unitarity gets violated by the former ansatz. The K-matrix provides a clear improvement compared to the Breit-Wigner parameterization, since two-body unitarity is built in. However, in general analyticity is violated. On the one hand, in the standard treatment not the full dispersive corrections are considered (in the expressions for the self energies only the imaginary parts and their analytic continuation are being kept and not the full expressions — c.f. Eq. (10) below), although some works include them (see, e.g., Ref. [6]), on the other hand, the left hand cuts are not treated properly — if they are included at all, in order to fit the scattering amplitudes, they are often in the same way included in the production amplitude although there the left hand cuts are different or, as in case of form factors, even absent.

To be specific, in this work we focus on form factors and scattering with the goal to present simple formulas that allow for a data analysis that is consistent with analyticity and unitarity, however, without the necessity to solve complicated integral equations. In addition, we present formulas that, by construction, in the low energy regime map smoothly and consistently onto what can be derived from the high accuracy analyses mentioned above and thus for the scattering even include the proper left hand cuts.

As an example and for demonstration we apply the formalism in this paper to the pion vector form factor, related to $\pi\pi$ scattering in the p -wave. The experimental situation for the ρ resonances beyond the $\rho(770)$ is at present not very clear: different experiments find indications for different resonances. While two resonances ($\rho(1450)$ and $\rho(1700)$) appear to be well established, 3 additional resonance candidates can be found in the literature — for a summary of the current situation see ‘note on the $\rho(1450)$ and the $\rho(1700)$ ’

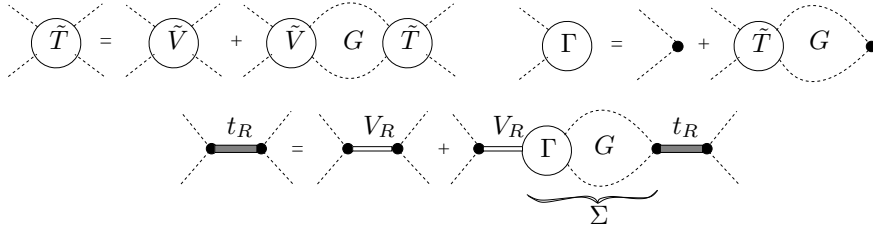


Fig. 1. Diagrammatic representation for the various ingredients of the formalism.

in the Review of Particle Physics [7]. The formalism presented here could be an important step forward to clarify the situation for it allows for a simultaneous, consistent analysis of various channels/observables.

As an example and for demonstration we apply the formalism in this paper to the pion vector form factor, related to $\pi\pi$ scattering in the p -wave. The experimental situation for the ρ resonances beyond the $\rho(770)$ is at present not very clear: different experiments find indications for different resonances — for a summary of the current situation see ‘note on the $\rho(1450)$ and the $\rho(1700)$ ’ in the Review of Particle Physics [7] — to parameterize the vector form factor beyond $s = 1 \text{ GeV}^2$ all studies agree on the need to include at least two resonances in addition to the $\rho(770)$, which is elastic. The formalism presented here could be an important step forward to clarify the situation for it allows for a simultaneous, consistent analysis of various channels/observables. The number of parameters needed for each resonance agrees to standard parameterizations. The advantage of the parameterization presented here is that we do not need to approximate the left hand cuts, the consistency with low energy phase shift is ensured by construction and the connection between scattering and form factors is properly implemented.

The paper is structured as follows: the most important formulas are motivated and presented in Sec. 2. Their more detailed derivation is given in Sec. 3. Results are presented in Sec. 5 and the paper closes with a short summary in Sec. 6. The two-potential formalism which forms the basis for the derivation is introduced in the Appendix.

2. Summary of most important results

The fundamental quantity in the current analysis is the pion vector form factor $F_V(s)$ defined via

$$\langle \pi^+(q_1)\pi^-(q_2)|J^\mu|0\rangle = (q_1 - q_2)^\mu F_V(s) , \quad (1)$$

where $s = (q_1 + q_2)^2$. For clarity in this paper we will only discuss $F_V(s)$, although the formalism is more general.

Below the first inelastic threshold only the two-pion channel needs to be considered. Then it is possible to give a closed form expression for the form factor F_V solely in terms of the elastic scattering phase shift — the so-called Omnès solution [8]. It is derived from a dispersion relation using the fact that

$$\text{disc}(F(s)) = 2i\sigma T(s)^* F(s) , \quad (2)$$

where T denotes the on-shell elastic scattering amplitude, and $\sigma = \sqrt{1 - 4m_\pi^2/s}/(48\pi)$ the two-body phase space. Here ‘disc’ denotes the discontinuity of the form factor defined via

$$\text{disc}(F_V(s)) = F_V(s + i\epsilon) - F_V(s - i\epsilon) = 2i\text{Im}(F) .$$

If the elastic phase shift is $\delta(s)$, with

$$T(s) = \frac{1}{\sigma} \sin(\delta(s))e^{i\delta(s)} , \quad (3)$$

then the form factor reads in the absence of bound states

$$F(s) = \Omega[\delta](s)P_A(s) \quad (4)$$

with the Omnès function

$$\Omega[\delta](s) = \exp \left\{ \frac{s}{\pi} \int_{4m^2}^{\infty} \frac{ds'}{s'} \frac{\delta(s')}{s' - s} \right\} . \quad (5)$$

where the function $P_A(s)$ is a polynomial. Its degree may be fixed by the large s behavior of the form factors. For values of $s < 1 \text{ GeV}^2$ this methodology was used by various authors for the pion vector form factor, see, e.g. Refs. [4,9–14].

In this letter a formalism is derived that

- smoothly maps onto Eqs. (3) and (4) for the elastic T matrix and the form factor respectively at low energies;
- is an analytically improved version of the well known K -matrix approach at higher energies;
- can be presented in closed form.

Especially Eqs. (3) and (4) will be replaced by

$$T(s)_{ij} = \delta_{ij}\delta_{1i}\tilde{T}(s) + T_R(s)_{ij} = \delta_{ij}\delta_{1i}\tilde{T}(s) + \xi_i\Gamma_{\text{out}}(s)_i t_R(s)_{ij} \Gamma_{\text{in}}(s)_j^\dagger \xi_j , \quad (6)$$

and

$$F(s)_i = \Gamma_{\text{out}}(s)_i [1 - V_R(s)\Sigma(s)]_{ik}^{-1} M_k , \quad (7)$$

with

$$\Gamma_{\text{out}}(s)_i = \Gamma_{\text{in}}(s)_i^\dagger = \begin{cases} \Omega[\tilde{\delta}](s) & \text{for } i = 1 \\ 1 & \text{otherwise} \end{cases}$$

and

$$\tilde{T}(s) = \frac{1}{\sigma_1} \sin(\tilde{\delta}(s)) e^{i\tilde{\delta}(s)} , \quad (8)$$

$$t_R(s)_{ij} = [1 - V_R(s)\Sigma(s)]_{ik}^{-1} V_R(s)_{kj} \quad (9)$$

and

$$\Sigma_i(s) = \frac{s}{\pi} \int_{s_{\text{thr } i}}^{\infty} \frac{ds'}{s'} \frac{\sigma_i(s') \xi_i^2 |\Gamma_i(s')|^2}{s' - s - i\epsilon} . \quad (10)$$

The resonance potential V_R as well as the production vertex M will be discussed in detail in the next section. The functions ξ_i (σ_i) parametrize the centrifugal barrier (phase space) operative in channel i — the concrete parametrization used will be given in the next section. In Fig. 1 a graphic representation of the various quantities is given.

Eq. (7) is the central result of our paper. If all vertex functions were chosen to be constant, it would reduce to the famous P -vector formalism [15]. However, since in our case Γ_1 , which enters explicitly in the expression for F_1 as well as through Σ_1 , is non-trivial, Eq. (7) provides a generalization to the conventional treatment.

The compared to Eq. (3) additional contribution to the T matrix, T_R , will be constructed such that it gets negligible at low energies, such that

$$T(s)_{ij} \simeq \delta_{ij}\delta_{1i}\tilde{T}(s) \text{ for } s < 1 \text{ GeV}^2 ,$$

and therefore we may identify $\tilde{\delta}(s)$ with the high accuracy phase shifts derived from, e.g., Roy equations mentioned in the introduction — see also Sec. 5. At the same time the non-analytic pieces embodied in $[1 - V_R(s)\Sigma(s)]_{ik}^{-1} M_k$ get heavily suppressed with the result that Eq. (7) maps onto Eq. (4) — the net effect of this term below $s = 1 \text{ GeV}^2$ is a 10% increase in the pion radius compared to what comes from Eq. (5), as demanded by the data. In the next section the equations are derived. Results are presented in Sec. 5.

3. Derivation of the Formalism

Eqs. (2) and (5) apply only, if the interactions are purely elastic — for the latter it is even necessary that they are elastic up to infinite energies. Clearly this is not realistic. However, experimental data show that at higher energies inelasticities are typically accompanied by resonances. We therefore split the full, partial wave projected interaction potential V into two pieces

$$V(s)_{ij} = \tilde{V}(s)_{ij} + V_R(s)_{ij} , \quad (11)$$

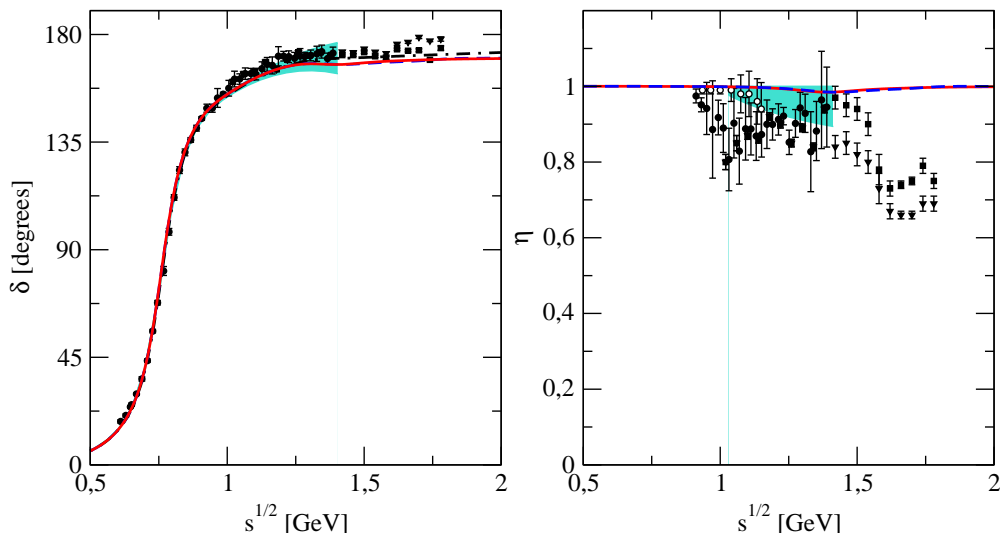


Fig. 2. Fits result for the pion p -wave phase shift (left panel) and inelasticity (right panel). The red solid band (blue dashed lines) denotes the result of the fit #2 (#1). The dot-dashed line in the left panel refers to the input phase $\tilde{\delta}$. Data are from Ref. [16] (solid dots — only data below 1.4 GeV are shown [17]), Ref. [18] (solid squares for solution (— —); solid triangles for solution (— + —)), and Ref. [19] (open dots) and Ref. [1] (turquoise band).

where i and j denote the channels. The crucial feature for this approach is that the potential \tilde{V} needs to be specified at no point. All what is needed are the corresponding phase shifts $\tilde{\delta}$. We now *postulate* the following properties:

- the potential \tilde{V} is purely elastic, such that \tilde{V} is non-vanishing only for $i = j = 1$;
- deviations in the $\pi\pi$ phase-shifts from $\tilde{\delta}$ come solely from s -channel resonances;
- all long ranged forces (driven by left-hand cuts) are in the elastic $\pi\pi$ interactions \tilde{V} ; all interactions in other channels are regarded as short ranged.

These are the model dependent assumptions of this approach (note, in case of the traditional isobar model one needs to assume that *all* interactions are mediated by s -channel resonances). Based on these Eqs. (2) and (5) can be easily generalized to multiple channels providing a convenient parameterization for both scattering as well as production amplitudes.

The full scattering T -matrix appears as the solution of a Bethe-Salpeter equation with input potential V defined in Eq. (11). Using the two potential formalism (see Ref. [20] and Appendix) it is straightforward to derive the decomposition given in Eq. (6).

The resonance potential may be written as (note: not all resonances are in V_R ; elastic resonances may be included in \tilde{T} — as the $\rho(770)$ in the example below)

$$\bar{V}_R(s)_{ij} = - \sum_{l=1}^n g_i^{(l)} G_{(l,\nu)} g_j^{(\nu)} ; \quad G_{(l,\nu)} = \frac{1}{s - m_{(l)}^2} \delta_{(l,\nu)} ; \quad V_R(s) = \bar{V}_R(s) - \bar{V}_R(0) . \quad (12)$$

In Fig. 1 a graphic representation of the various quantities is given. The potential is subtracted once at $s = 0$ to ensure that the phase of the full T matrix at low energies agrees to the input phase $\tilde{\delta}$. Clearly, the procedure does not guarantee a priori that the phase of the full T -matrix is close to that of \tilde{T} in the whole range where \tilde{T} is well determined, however, in practice this is indeed the case: as can be seen from the left panel of Fig. 2, at energies below 1 GeV all curves shown, including that for the input phase shift, are indistinguishable. In this sense a single subtraction is sufficient for the consistency of the approach and therefore higher subtractions are not necessary.

The M_i denote point like source terms for the production of particles into channel i . It may be written as

$$M_k = c_k - \sum_{l=1}^n g_i^{(l)} G_{(l,\nu)} \alpha^{(\nu)} s . \quad (13)$$

Note, as a consequence of gauge invariance we use a photon–resonance coupling linear in s ¹. This coupling at the same time suppresses the influence of heavier resonances on the low s region. The parameters c_k allow for a direct transition of the photon to the different continuum channels. In case of the pion vector form factor, discussed in detail below, charge conservation demands $c_1 = 1$, the other c_k are free parameters of the fit. This is in contrast to the isobar model, where commonly only resonant interactions are allowed, however, these kinds of couplings appear naturally in more microscopic approaches [21–24].

The centrifugal barrier factor in the two–pion channel is given by

$$\xi_1 = \sqrt{s - 4m_\pi^2}^{L_1} \left(\frac{\lambda^2}{\lambda^2 + s} \right) \quad (14)$$

with L_1 for the angular momentum of the pion pair. The final factor on the right hand side is introduced to tame the growth of ξ_1 that comes from the centrifugal barrier factor. In this work λ is not treated as a parameter determined by the fit, but we will vary its value within some ranges and use the variation in the fit results as some estimate for systematic uncertainties. Note: all channels discussed explicitly here have $L_i = 1$, however, e.g. the ρf_0 channel couples to the $\pi\pi$ vector channel in an even partial wave.

To parameterize the inelastic channels we use for $i = 2$ a structureless 4π channel via the phase space factor $\sigma_2 = \sqrt{1 - 16m_\pi^2/s}^7 / (48\pi)$, which provides the proper scaling of the four–body phase space near the threshold. For the barrier factor we use $\xi_2 = \sqrt{s - 16m_\pi^2} [\lambda^2 / (\lambda^2 + s)]$. Although the $\bar{K}K$ channel contributes significantly to isoscalar $\pi\pi$ interactions, it gives negligible contributions in the isovector channel [25]. Therefore we include as additional inelastic channel ($i = 3$) the $\pi\omega$ channel. For a discussion on the possible role of the $\pi\omega$ channel on the $\pi\pi$ inelasticity see Ref. [26,27]. We take $\sigma_3 = \sqrt{(s - (m_\omega + m_\pi)^2)(s - (m_\omega - m_\pi)^2)} / s / (48\pi)$ and $\xi_3 = 48\pi\sigma_3s[\lambda^2 / (\lambda^2 + s)]$.

It is straightforward to show that the imaginary parts of the self–energies read (see Appendix)

$$\text{Im}(\Sigma_i(s)) = \sigma_i \xi_i^2 |\Gamma_i(s)|^2 \theta[s - s_{\text{thri}}] , \quad (15)$$

where $\theta[\dots]$ denotes the step function equal to 1 (0) for positive (negative) arguments. Thus the self energies can be calculated from a properly subtracted dispersion integral. Since $\Sigma(s_0)$ at some s_0 can be absorbed into the resonance masses we here use a once subtracted version — c.f. Eq. (10). The resulting self energies $\Sigma_1(s)$, $\Sigma_2(s)$, and $\Sigma_3(s)$ are shown in left, middle and right panel of Fig. 3, respectively. In all panels the solid lines refer to the imaginary parts while the dashed lines refer to the real parts. The rise of the imaginary part of both Σ_2 and Σ_3 comes from the centrifugal barrier terms ξ_2 and ξ_3 , respectively, its curvature comes from the vertex function $\lambda^2 / (s + \lambda^2)$. Each panel contains three curves of each kind: the most strongly curved ones come from $\lambda = 4$ GeV, the least curved one from $\lambda = 6$ GeV, while the middle one refers to $\lambda = 5$ GeV.

To calculate the form factor we may write (using the symbolic notation of the Appendix)

$$\xi F = \xi M + T G \xi M , \quad (16)$$

where G_i is the operator representation for the integration over all intermediate n –body states of channel i and the production vertices M_i were defined in Eq. (13). Note the appearance of the centrifugal barrier factors in Eq. (16). They appear, since the discontinuity equations are derived on the basis of the full transition current that, in addition to the form factor, contains a kinematic factor for pion pairs in a partial wave higher than s –wave — see Eq. (1). Inserting Eq. (6) into Eq. (16), we get, after deviding by ξ_i

$$F_i = M_i + \tilde{T}_{ij} G_j (\xi_j / \xi_i) M_j + (T_R)_{ij} G_j (\xi_j / \xi_i) M_j = \Gamma_{\text{out}i} (\delta_{ij} + (t_R)_{ij} \Gamma_{\text{in}j}^\dagger G_j \xi_j^2) M_j .$$

To proceed we may use the definition of the self energy, $\Sigma_i = \Gamma_{\text{in}i}^\dagger G_i \xi_i^2$, to write

$$t_R \Sigma = [1 - V_R \Sigma]^{-1} V_R \Sigma = -1 + [1 - V_R \Sigma]^{-1} .$$

Here we needed to assume that the range of interactions in the production vertex and in the vertex functions of the resonances is similar in all channels, for only then the same loop integral Σ_i can be used as self energy

¹ On the Lagrangian level this means a coupling of the resonance to the photon field via $F^{\mu\nu} \partial_\mu V_\nu$ with $F^{\mu\nu}$ for the electromagnetic field strength tensor and V_ν for the resonance field.

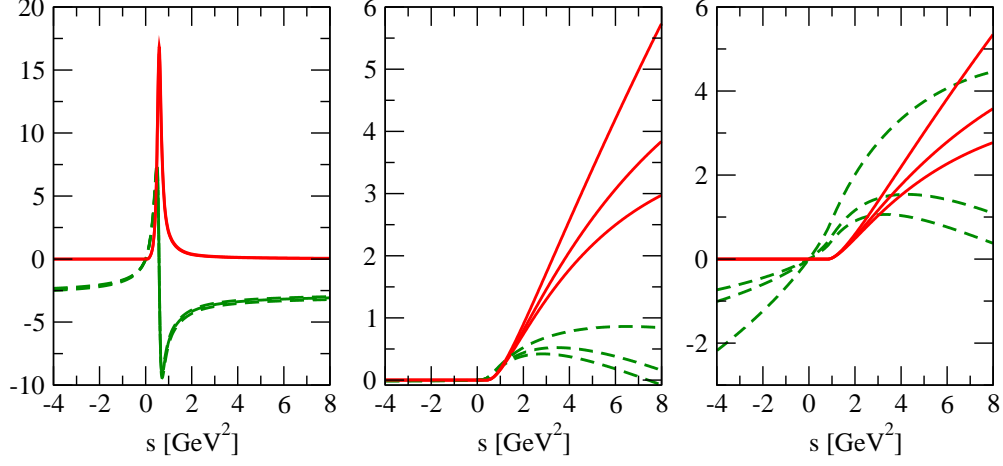


Fig. 3. Real and imaginary parts for the self energies $\Sigma_i(s)$ defined in Eq. (10). The solid (dashed) lines show the imaginary (real) part. The left, middle and right panel refer to the self energies from the 2π , 4π and $\pi\omega$ channels. The different curves refer to different values of the cut-parameter λ in the vertex functions as described in the text.

contribution for the resonances as well as convolution integral of M_i and the resonance potential. From this we get

$$F = \Gamma_{\text{out}} [1 - V_R \Sigma]^{-1} M ,$$

which agrees to Eq. (7).

It is important to observe that the expression given in Eq. (7) is consistent with the coupled channel version of the unitarity relation for form factors, Eq. (2), since

$$\begin{aligned} \text{disc}(F_1) &= \text{disc}(\Gamma_{\text{out}1}) [1 - V_R \Sigma]_{1j}^{-1} M_j + \Gamma_{\text{out}1}^* \text{disc}([1 - V_R \Sigma]^{-1})_{1j} M_j \\ &= 2i \tilde{T}^* \sigma_1 \Gamma_{\text{out}1} [1 - V_R \Sigma]_{1j}^{-1} M_j + \Gamma_{\text{out}1}^* ([1 - V_R \Sigma^*]^{-1} V_R)_{1k} \text{disc}(\Sigma)_k [1 - V_R \Sigma]_{kj}^{-1} M_j \\ &= 2i \left(\tilde{T}^* \delta_{1k} + \xi_1 \Gamma_{\text{out}1}^* (t_R)_{ik} \Gamma_{\text{out}k}^* \xi_k \right) \sigma_k (\xi_k / \xi_1) \Gamma_{\text{out}k} [1 - V_R \Sigma]_{kj}^{-1} M_j \\ &= 2i T_{1k}^* \sigma_k (\xi_k / \xi_1) F_k \end{aligned} \quad (17)$$

where in the intermediate step the unitarity relation for the vertex function, Eq. (2), and the self energy, Eq. (15), were used.

An interesting observable is the ratio r of the total cross section for e^+e^- annihilation into hadronic states with $I = 1$ other than $\pi^+\pi^-$ over $\sigma_{e^+e^- \rightarrow \pi^+\pi^-}$ — a compilation of this quantity can be found in Ref. [25]. In this ratio the unitarization effects in the resonance T -matrix cancel largely. For example, in case of only one inelastic channel we get

$$r = \left| \frac{\left(\frac{\xi_2 \sigma_2 \Gamma_{\text{out}2}}{\xi_1 \sigma_1 \Gamma_{\text{out}1}} \right) \frac{(1 - V_{R11} \Sigma_1) M_2 + V_{R12} \Sigma_1 M_1}{(1 - V_{R22} \Sigma_2) M_1 + V_{R12} \Sigma_2 M_2}}{\left(\frac{\xi_2 \sigma_2 \Gamma_{\text{out}2}}{\xi_1 \sigma_1 \Gamma_{\text{out}1}} \right) \frac{(1 - V_{R11} \Sigma_1) M_2 + V_{R12} \Sigma_1 M_1}{(1 - V_{R22} \Sigma_2) M_1 + V_{R12} \Sigma_2 M_2}} \right|^2 , \quad (18)$$

clearly being very directly sensitive to the resonance parameters.

4. Inclusion of isospin violation

The vector form factor in the two pion channel is directly accessible from two reactions, namely from e^+e^- -annihilation and from τ decays. In the former case, in addition to what was discussed so far, isospin violating mechanisms need to be included.

There are two well established effects — $\rho - \omega$ and $\rho - \phi$ mixing. Both are visible as narrow structures in the pion vector form factor located at the masses of the ω and ϕ , respectively (c.f. inlays in Fig. 4). The inclusion of these mixings in the present formalism is straight forward — we here use a slightly modified version to what is used in Ref. [12], namely, for the neutral, $\pi^+\pi^-$, channel

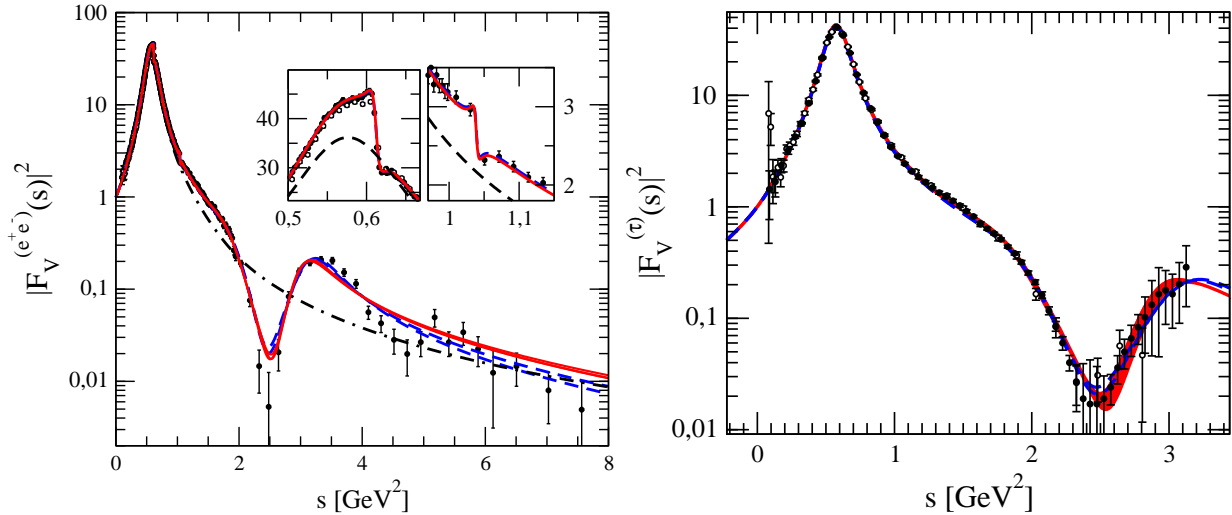


Fig. 4. Fit result for the pion vector form factor F_V . Left panel: For the neutral channel — the left (right) inlay shows a zoom to the region where ρ - ω (ρ - ϕ) mixing is visible. The red solid band (blue dashed lines) denotes the result of fit #1 (#2). The black dot-dashed line shows the form factor derived from the Omnès function only. Data are from the reaction $e^+e^- \rightarrow \pi^+\pi^-$ presented in Refs. [28,29]. Right panel: For the charged channel. Data are from Belle [30] and CLEO [31].

$$c_1 \longrightarrow c_1 \left(1 + \kappa_1 \frac{s}{s - m_\omega^2 + im_\omega \Gamma_\omega} + \kappa_2 \frac{s}{s - m_\phi^2 + im_\phi \Gamma_\phi} \right). \quad (19)$$

We here use $m_\omega = 0.7826$ GeV, $\Gamma_\omega = 0.0085$ GeV, $m_\phi = 1.0193$ GeV, and $\Gamma_\phi = 0.0043$ GeV. The strength parameters κ_i are part of the fit.

In Refs. [22] it was pointed out that in the form factor for the neutral channel the mixing with the photon needs to be taken into account as well. In Refs. [22] only the mixing with the $\rho(770)$ was considered. Here the photon can also mix with the higher resonances. The complete effect can be included via

$$\bar{V}_R^{EM}(s)_{ij} = - \sum_{l,l'}^n \hat{g}_i^{(l)} G_{(l,l')}^{EM} \hat{g}_j^{(l')} ; \quad V_R(s)_{ij} = \bar{V}_R(s)_{ij} - \bar{V}_R(0)_{ij} - \frac{e^2 c_i c_j}{s}. \quad (20)$$

and

$$M_k = c_k - \sum_{l=1}^n \hat{g}_i^{(l)} G_{(l,l')}^{EM} \alpha^{(l')} s, \quad (21)$$

with

$$\hat{g}_i^{(l)} = g_i^{(l)} - e^2 \alpha^{(l)} c_i. \quad (22)$$

The resonance propagators G^{EM} come from mixing of the hadronic resonance basis with the photon and are defined via

$$G^{EM} = [1 - G s \alpha \alpha^T]^{-1} G, \quad (23)$$

where the bare propagators G were defined in Eq. (12). Thus the mixing with the photon does not introduce any new parameter. For simplicity we do not include the additional isospin violating effects listed in Ref. [22].

5. Results for the pion phases, inelasticities and form factors in the p -wave

All parameters introduced — κ_i , c_i , $g_i^{(l)}$, $\alpha^{(l)}$, $m_{(l)}$ — are real as long as all (relevant) channels are treated explicitly as a consequence of time reversal invariance. In case of N channels, for each explicit resonance we need to include $N + 2$ real parameters. This number agrees exactly to what is needed, e.g., in the K matrix formalism. In addition there are the $N - 1$ direct couplings of the photon to the continuum channels, c_i — charge conservation fixes $c_1 = 1$. For the predominantly elastic resonance $\rho(770)$, which is included

fit	$\kappa_1 \times 10^3$	$\kappa_2 \times 10^3$	c_2	c_3	$m_{(1)}$	$m_{(2)}$	$g_1^{(1)}$	$g_2^{(1)}$	$g_3^{(1)}$	$g_1^{(2)}$	$g_2^{(2)}$	$g_3^{(2)}$	$\alpha^{(1)}$	$\alpha^{(2)}$
#1A	-2.2(1)	-0.6(1)	-4.9(2)	–	1.53(1)	2.3(1)	-1.40(3)	-38(1)	–	1.9(1)	114(10)	–	-0.04(1)	0.39(1)
#1B	-2.2(1)	-0.5(1)	4.5(1)	–	1.52(1)	2.4(1)	1.38(2)	-36(1)	–	-1.8(1)	120(1)	–	0.04(1)	-0.36(1)
#2A	-2.2(1)	-0.6(1)	3.8(1)	-6.2(4)	1.57(1)	2.0(1)	1.6(1)	-50(3)	2.8(7)	1.1(1)	-43(7)	14(2)	-0.01(20)	0.73(7)
#2B	-2.2(1)	-0.6(1)	3.6(1)	-5.8(4)	1.58(1)	2.0(1)	-1.6(1)	51(2)	-1.4(6)	0.9(1)	-37(5)	11(1)	0.01(10)	0.77(7)
#2C	-2.1(1)	-0.5(1)	3.6(3)	-5.5(4)	1.58(2)	2.0(1)	-1.6(1)	50(3)	-0.8(6)	0.8(1)	-37(5)	11(1)	-0.01(10)	0.8(1)

Table 1

Fit parameters for the various fits. The uncertainties listed refer to the statistical uncertainty of the individual fits only. Masses and α_i are given in GeV and GeV^{-2} , respectively; all other couplings are dimensionless. Fit #1A and #2A refer to $\lambda = 4$ GeV, #1B and #2B to 5 GeV and #2C to 6 GeV, as described in the text.

via $\tilde{\delta}$, the only free parameters are the mixing parameters κ_1 and κ_2 . Denoting the number of resonances included explicitly by n (c.f. Eq. (12)), we thus have $[(n+1)(N+2)-1]$ parameters in total. In this paper we discuss two classes of fits: one including 2 resonances and 2 channels, the other including 2 resonances and 3 channels. Thus, in the former case we have 11 in the latter 14 parameters to be adjusted to the data.

The resonance parameters will be determined by a fit to data on the time-like pion vector form factor as well as inclusive data on inelastic channels. All fits were performed using the MINUIT package of the CERN library. As input we need the elastic phase shifts $\tilde{\delta}$, which largely fix the properties of the $\rho(770)$.

For the input phase shifts $\tilde{\delta}$ we will use for energies below $s_{\text{cut}} = 1.4^2 \text{ GeV}^2$ the central values for the phase shift provided in Ref. [1] — see Eqs. (A7) and (A8) therein. For energies above this value we smoothly extrapolate the phase shift to a value of π via

$$\tilde{\delta}(s) = \pi + (\tilde{\delta}(s_{\text{cut}}) - \pi) \left(\frac{\Lambda^2 + s_{\text{cut}}}{\Lambda^2 + s} \right). \quad (24)$$

It turns out that for $\Lambda \geq 2 \text{ GeV}$ the results in the time like region are basically insensitive to the actual value used ². We thus chose $\Lambda = 10 \text{ GeV}$ in what follows. The asymptotic value π for the phase ensures that the vertex function $\Gamma_1(s)$ decreases as $1/s$ as demanded for the vector form factor. The resulting elastic $\pi\pi$ phase shifts are shown as the black dot-dashed line in the left panel of Fig. 2. The form factor from the Omnés function alone is shown as the black dot-dashed line in Figs. 4. It provides an acceptable description of the data up to $s = 1 \text{ GeV}^2$, although there are some deviations visible (see inlays in the left panel). At higher energies a significant deviation becomes visible.

The pion vector form factor shows pronounced structures for $s > 1.2 \text{ GeV}^2$ (c.f. Fig. 4). These call for the inclusion of at least two resonances. Resonances come with pronounced phase motions that are, however, not visible in the $\pi\pi$ phase shifts (c.f. Fig. 2). Therefore at least one inelastic channel needs to be included, for then this phase motion can appear in the phase of the form factor only; see discussion below. For this channel we choose a structure less 4π channel — the corresponding fits we call Fit #1. It turns out that in order to get the overall scale of the cross section ratio r right a non-vanishing value for the parameter c_2 , defined in Eq. (13), is needed. In order to investigate the model dependence of the parametrization we performed fits with different cut-off parameter λ in the vertex functions (c.f. Eq. (14)). If the dynamics considered explicitly in the model is sufficient to describe the physics in the energy range studied, one would expect a very mild dependence of the calculated observables on λ . This is indeed what is found when λ is varied between 4 and 5 GeV, however, for larger values of λ a simultaneous fit to F_V and r was not possible. The blue dashed lines in Figs. 2, 4 and 5 for phases and inelasticities, the pion vector form factor from e^+e^- annihilation and τ decays, and the ratio r , respectively, show the fit results for $\lambda = 4$ (fit #1A) and 5 (fit #1B). The corresponding parameters are given in Table 1.

Since the allowed range of variation of λ was limited and since the energy dependence of the ratio r is not well described with only one inelastic channel, we performed a second group of fits with the $\omega\pi$ channel included in addition. Now λ can be varied over a larger range — the red band in Figs. 2, 4 and 5 reflects the variation of the fit results when λ is changed from 4 GeV (fit #2A) to 6 GeV (fit #2C) — even for $\lambda = 10$

² This is correct up to an unphysical pole located at $s = -\Lambda^2$, which, however, does not influence visibly the amplitude for $s > -\Lambda^2$.

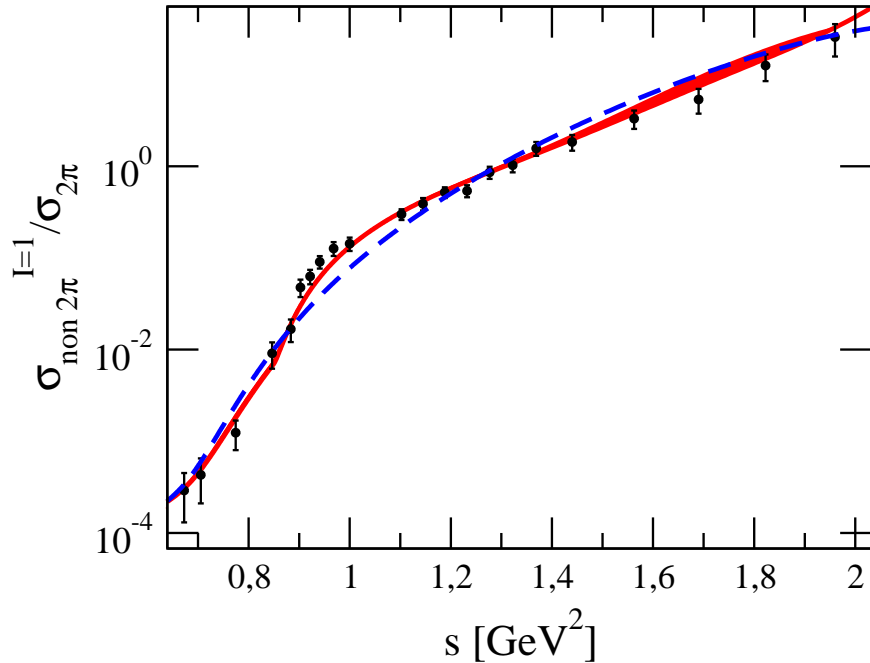


Fig. 5. Results for the ratio $r = \sigma_{e^+e^- \rightarrow (\text{non}2\pi)}^{I=1} / \sigma_{e^+e^- \rightarrow \pi^+\pi^-}$. The red solid band (blue dashed lines) denotes the result of the fits #2, (#1). Data are from the compilation of Ref. [25].

GeV a reasonable fit can be found with slightly larger χ^2 . The parameters extracted from the fits are listed in Table 1.

In case of the pion vector form factor we fit to the BaBar data on e^+e^- annihilation only, for it extends to higher energies³. Especially, neither the space like form factor data nor the τ data were included in the fit — the result comes out as a prediction. The parameters determined in both fits are given in Tab. 1. It is important to note that for the pion vector form factor alone both fits are of similar quality: for fit #1 and #2 we have $\chi^2/d.o.f=1.2$ and 1.4, respectively. However, only fit #2 provides an acceptable description for r . This result nicely illustrates that one should not analyze the pion vector form factor without looking at the non 2π channels at the same time. Note that at $s = 2 \text{ GeV}^2$ Ref. [25] reports a value of $r \sim 26$, which shows that already at this relatively low energy the 2π channel provides only a small fraction of the e^+e^- annihilation rate in the $I = 1$ channel.

The s dependence of the non 2π data shown in Fig. 5 calls at least for two inelastic channels, since there is a change in slope visible at around $s \sim 0.9$. In fit #2 this is accounted for by the inclusion of the $\pi\omega$ channel. However, even this three channel fit is still too simplified, for there should be not only correlations amongst the 4 pions in channel 2 included, e.g. from $a_1\pi$, $\rho\rho$, and $\rho\sigma$. In addition there are also channels like $\eta\pi\pi$. The data included in the current study does not allow one to disentangle these and therefore to improve the description of r further. What is necessary is an inclusion of the large number of exclusive measurements available from e^+e^- annihilation. We leave this to a future study.

In contradistinction to most approaches in this model direct couplings of the photon to the continuum channels are included; all fits called for non-zero values of these (c.f. Tab. 1). However, the same effect could also be achieved by inclusion of a heavy ($m > 4 \text{ GeV}$) resonance. In order to decide if the dynamics included here is sufficient a fit to more, exclusive data is compulsory. It is important to stress that the mass parameters given in the table are bare parameters that get renormalized by the self energies. It is therefore possible that the lowest resonance poles come out very close in both fits, for the unitarization effects are

³ In this exploratory study we regard this as appropriate since in this work we do not perform an uncertainty estimate of the parameters extracted.

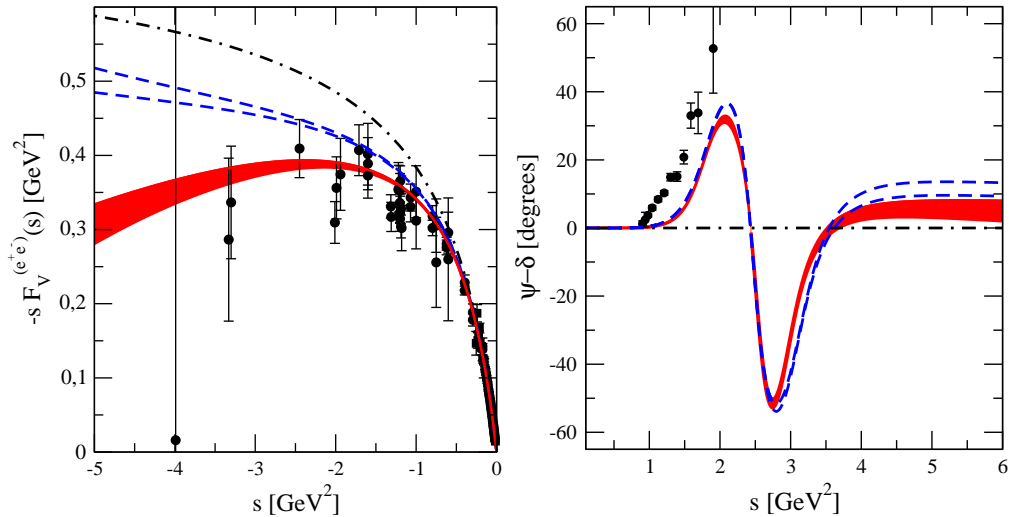


Fig. 6. Left panel: Fit result for the pion vector form factor at space-like energies. The lines are the same as in Fig. 4. Data are from Ref. [32,33]. Right panel: phase difference between ψ , the phase of the form factor, and the scattering phase shift δ . The data shown indicate the upper bound of the phase shift difference presented in Ref. [25].

different. However, we postpone the determination of pole positions, which requires the evaluation of the elastic T -matrix \bar{T} in the complex plane, to a later work.

A direct $\rho\pi\omega$ coupling was shown to be significant, e.g., in [34]. The information how strong this transition is in the present approach is contained in the values of the corresponding residue at the $\rho(770)$ pole, however, to get access to this also calls for an analytic continuation of the amplitudes into the complex plane.

The results of the two fits for the vector form factor at space-like energies are shown in the left panel of Fig. 6. Both lead to a pion radius slightly enhanced compared to what comes from the Omnès function itself, shown by the dot-dashed line: through the inclusion of the high-lying resonances the mean square charge radius of the pion increases by nearly 10% from 0.40 fm^2 to 0.44 fm^2 . The latter value is consistent with the values extracted in Refs. [35,36]. For the curvature we find $c_V = 3.9 \text{ GeV}^{-4}$, in line with Refs. [14,37]. The effect of the higher resonances is quantitatively in line with expectations from dimensional analysis that predicts an effect on the mean square radius of order of the square of the inverse resonance mass $\sim 0.02 \text{ fm}^2$. At higher space like energies the results of both fits are consistent with the largely model independent bounds for the form factor derived in Ref. [38], while the form factor from the Omnès function is inconsistent.

The left panel of Fig. 2 nicely illustrates that within the formalism presented the high accuracy phase shifts up to 1 GeV are reproduced very well. One also finds that the phase shifts for the full model largely agree to the input phase in the whole energy range considered (this is not the case for the phase of the form factor, as discussed in the next paragraph) as well as to the data of Ref. [16,18]⁴. This happens, since the resonance couplings to the $\pi\pi$ channel are rather small — the resonances show up prominently in the form factor mainly due to the couplings to the photon. Especially, the present model can not account for the significant inelasticity visible in the data of Ref. [18] — the according to Ref. [39] preferred solution $(-+-)$ shows an inelasticity of the 0.8 already at 1 GeV. At this point in time it is not possible to decide whether this failure is an indication of a short coming of the model used here, or of the data of Refs. [16,18]. What might support the latter conjecture is that the data on η of Refs. [16,18] are in disagreement with both the analysis of Ref. [19] as well as that of Ref. [1] at around 1 GeV.

In the elastic regime the phase of the form factor has to agree to the phase of elastic scattering — a fact known as Watson theorem [40]. At higher energies this connection is lost. In the right panel of Fig. 6 we show the difference between ψ , the phase of the form factor, and the scattering phase shift δ . Also shown in the panel is the allowed upper bound of the phase shift difference given in Ref. [25]. As one can see our

⁴ Only two of the 4 solutions presented in that paper are given, for the other two are in strong discrepancy with the phase shifts of Ref. [1].

amplitudes largely exhaust the range allowed by unitarity. This reflects again the fact that in the present formalism all resonances besides the $\rho(770)$ couple to the $\pi\pi$ channel only weakly.

6. Summary and Outlook

In this paper a formalism was presented that allows for a simultaneous description of both $\pi\pi$ scattering data as well as form factors without the need to model the low energy regime: at low energies $\pi\pi$ phases can be used as input directly. At higher energies the formalism maps smoothly onto the well known N/D method which is similar to the K -matrix approach, however, with improved analytical properties. As an example in this paper the formalism was applied to pion pairs in the p -wave. An excellent description is found for the pion vector form factor in both the neutral channel — from e^+e^- annihilations, with ρ - ω and ρ - ϕ and resonance- γ mixing included — as well as the charged channel — from τ decays. In addition we also found a qualitative agreement with data on the non 2π channels from e^+e^- annihilations — these data were studied within a dynamical model here for the first time.

We found, however, that within the given formalism it was not possible to describe the behavior of the inelasticity given in Refs. [16,18]. At this point in time we are not able to judge if this deviation indicates a short coming of the model or points at a problem in the data. However, the observation that the values of η of Refs. [16,18] are in disagreement with the analyses of Refs. [1,19] at $s \sim 1 \text{ GeV}^2$ might indicate that there is a problem in the data of Refs. [16,18] also at higher energies.

The formalism described here can be applied to all partial waves, especially also the isoscalar s -wave. Here, however, it is less clear what to use for the elastic phase shift $\tilde{\delta}$, since the pronounced structure from the $f_0(980)$, which also couples strongly to $\bar{K}K$, shows up already short after the phase reached 90° . We leave this study to a future work.

Acknowledgment

I thank Maurice Benayoun, Irinel Caprini, Simon Eidelman, Martin Hoferichter, Bastian Kubis, Ulf-G. Meißner and Juan M. Nieves for useful and inspiring discussions and comments to the manuscript and Wolfgang Ochs for useful remarks about the data of Refs. [16,18].

Appendix A. The two potential formalism

Let us assume that there is a sensible way to split the scattering potential into two pieces (as in the main text the potentials \tilde{V} and V_R , the vertex function Γ as well as the T -matrices are matrices in channel space, while the form factor F and the production vertices M are vectors in channel space)

$$V = \tilde{V} + V_R .$$

We will show in this Appendix that the full T -matrix can be split accordingly — to simplify notations, in the appendix we do not show the centrifugal barrier factors ξ explicitly. In operator form the Bethe–Salpeter equation for the T matrix may be written as

$$T = V + VGT = \tilde{V} + V_R + (\tilde{V} + V_R)GT .$$

Here G_i denotes the operator for the integral over the n -particle intermediate state of channel i , e.g. for the two- π intermediate state we have

$$VGV \propto \frac{1}{i} \int \frac{d^4k}{(2\pi)^4} V(k, \dots) \frac{1}{k^2 - m^2 + i\epsilon} \frac{1}{(k - P)^2 - m^2 + i\epsilon} V(k, \dots) ,$$

where P denotes the total 4-momentum of the system, $P^2 = s$. Note, not all arguments of the potential V are shown explicitly. Introducing \tilde{T} as the solution of

$$\tilde{T} = \tilde{V} + \tilde{V}G\tilde{T}$$

and the dressed vertex functions

$$\Gamma_{\text{out}} = 1 + \tilde{T}G \quad \text{and} \quad \Gamma_{\text{in}}^\dagger = 1 + G\tilde{T}$$

we get

$$T = \tilde{T} + T_R = \tilde{T} + V_R \Gamma_{\text{in}}^\dagger + (V_R G + \tilde{V}G)T_R .$$

Due to time reversal invariance we have $\Gamma_{\text{out}} = \Gamma_{\text{in}}^\dagger$. Since $\text{disc}(G)=2i\sigma$ and $\text{disc}(\tilde{T}) = 2i\sigma\tilde{T}^*\tilde{T}$ one has

$$\text{disc}(\Gamma_{\text{out}}(s)) = \text{disc}(\tilde{T})G + \tilde{T}^*\text{disc}(G) = \sigma\tilde{T}(s)^*\Gamma_{\text{out}}(s) ,$$

thus Γ_{out} holds the unitarity relation for a form factor in a channel where the interactions are given by \tilde{T} .

We may therefore define

$$T_R = \Gamma_{\text{out}} t_R \Gamma_{\text{in}}^\dagger$$

and derive with $\Sigma = G\Gamma_{\text{out}}$ and $\tilde{V}G\Gamma_{\text{out}} = \Gamma_{\text{out}} - 1$

$$t_R = V_R + V_R \Sigma t_R \quad \longrightarrow \quad t_R = [1 - V_R \Sigma]^{-1} V_R .$$

From the definition above the discontinuity of the self-energy Σ is found to be

$$\text{disc}(\Sigma) = \text{disc}(G)\Gamma_{\text{out}} + G^*\text{disc}(\Gamma_{\text{out}}) = 2i \underbrace{\left(1 + G^*\tilde{T}^*\right)}_{\Gamma_{\text{out}}^*} \sigma \Gamma_{\text{out}} ,$$

which was used to derive Eq. (10).

References

- [1] R. Garcia-Martin et al., Phys. Rev. D **83** (2011) 074004 [arXiv:1102.2183 [hep-ph]].
- [2] G. Colangelo, J. Gasser and H. Leutwyler, Nucl. Phys. B **603** (2001) 125 [hep-ph/0103088].
- [3] G. J. Gounaris and J. J. Sakurai, Phys. Rev. Lett. **21** (1968) 244.
- [4] M. F. Heyn and C. B. Lang, Z. Phys. C **7** (1981) 169.
- [5] H. Czyz, A. Grzelinska and J. H. Kuhn, Phys. Rev. D **81** (2010) 094014.
- [6] A. V. Anisovich et al., Phys. Rev. D **84** (2011) 076001.
- [7] K. Nakamura *et al.* [Particle Data Group Collaboration], J. Phys. G G **37** (2010) 075021.
- [8] R. Omnes, Nuovo Cim. **8** (1958) 316.
- [9] J. Gasser and U.-G. Meißner, Nucl. Phys. B **357** (1991) 90.
- [10] F. Guerrero, Phys. Rev. D **57** (1998) 4136 [arXiv:hep-ph/9801305]; F. Guerrero and A. Pich, Phys. Lett. B **412** (1997) 382 [arXiv:hep-ph/9707347].
- [11] A. Pich and J. Portoles, Phys. Rev. D **63** (2001) 093005 [hep-ph/0101194].
- [12] J. F. De Troconiz and F. J. Yndurain, Phys. Rev. D **65** (2002) 093001 [hep-ph/0106025].
- [13] F. Guerrero and J. A. Oller, Nucl. Phys. B **537** (1999) 459 [Erratum-ibid. B **602** (2001) 641] [hep-ph/9805334].
- [14] F. -K. Guo et al., Phys. Lett. B **678**, 90 (2009) [arXiv:0812.3270 [hep-ph]].
- [15] I. J. R. Aitchison, Nucl. Phys. A **189** (1972) 417.
- [16] B. Hyams et al., Nucl. Phys. B **64** (1973) 134.
- [17] W. Ochs, private communication. See also Ref. [18].
- [18] B. Hyams et al., Nucl. Phys. B **100** (1975) 205.
- [19] S. D. Protopopescu et al., Phys. Rev. D **7** (1973) 1279.
- [20] K. Nakano, Phys. Rev. C **26** (1982) 1123.
- [21] M. Benayoun et al., Phys. Rev. D **59** (1999) 114027
- [22] F. Jegerlehner and R. Szafron, Eur. Phys. J. C **71** (2011) 1632
- [23] C. Terschlusen and S. Leupold, Phys. Lett. B **691** (2010) 191.
- [24] M. Benayoun, P. David, L. DelBuono and F. Jegerlehner, Eur. Phys. J. C **72** (2012) 1848
- [25] S. Eidelman and L. Lukaszuk, Phys. Lett. B **582**, 27 (2004) [hep-ph/0311366].
- [26] B. Costa de Beauregard, et al., Phys. Lett. B **67** (1977) 213.
- [27] F. Niecknig, B. Kubis and S. P. Schneider, arXiv:1203.2501 [hep-ph].
- [28] B. Aubert *et al.* [BABAR Collaboration], Phys. Rev. Lett. **103** (2009) 231801 [arXiv:0908.3589 [hep-ex]].
- [29] F. Ambrosio *et al.* [KLOE Collaboration], Phys. Lett. B **700** (2011) 102 [arXiv:1006.5313 [hep-ex]].
- [30] M. Fujikawa *et al.* [Belle Collaboration], Phys. Rev. D **78** (2008) 072006 [arXiv:0805.3773 [hep-ex]].
- [31] S. Anderson *et al.* [CLEO Collaboration], Phys. Rev. D **61** (2000) 112002 [hep-ex/9910046].
- [32] S.R. Amendolia *et al.* [NA7 Collaboration], Nucl. Phys. B **277** (1986) 168.

- [33] G. M. Huber *et al.* Phys. Rev. C **78** (2008) 045203; H. Ackermann *et al.*, Nucl. Phys. B **137** (1978) 294. J. Volmer *et al.* Phys. Rev. Lett. **86** (2001) 1713; C. J. Bebek *et al.*, Phys. Rev. D **17** (1978) 1693.
- [34] M. Gell-Mann, D. Sharp and W. G. Wagner, Phys. Rev. Lett. **8** (1962) 261.
- [35] F. Stollenwerk *et al.*, Phys. Lett. B **707** (2012) 184 [arXiv:1108.2419 [nucl-th]].
- [36] G. Colangelo, Nucl. Phys. Proc. Suppl. **131** (2004) 185 [hep-ph/0312017].
- [37] G. Abbas, B. Ananthanarayan and S. Ramanan, Eur. Phys. J. A **41** (2009) 93 [arXiv:0903.4297 [hep-ph]].
- [38] B. Ananthanarayan, I. Caprini and I. S. Imson, arXiv:1203.5398 [hep-ph].
- [39] W. Ochs, Nucl. Phys. Proc. Suppl. **174** (2007) 146 [hep-ph/0609207].
- [40] K. M. Watson, Phys. Rev. **95** (1954) 228.